Impact of Li2O2 particle size on Li–O2 battery charge process: insights from a multiscale modeling perspective

Yinghui Yin, Caroline Gaya, Amangeldi Torayev, Vigneshwaran Thangavel, Alejandro A. Franco

Impact of Li_2O_2 Particle Size on Li–O_2 Battery Charge Process: Insights from a Multiscale Modeling Perspective

Yinghui Yin,[†,‡] Caroline Gaya,[†,§] Amangeldi Torayev,[†,∥] Vigneshwaran Thangavel,[†,‡] and Alejandro A. Franco*[,†,‡,∥]

[†]Laboratoire de Réactivité et Chimie des Solides (LRCS), CNRS UMR 7314, Université de Picardie Jules Verne, 33 rue St. Leu, 80039 Amiens, France

[‡]Réseau sur le Stockage Electrochimique de l'Energie (RS2E), Fédération de Recherche CNRS 3459, 33 rue St. Leu, 80039 Amiens, France

[§]IRT Saint-Exupery, 118 route de Narbonne, 31432 Toulouse, France

[∥]ALISTORE-European Research Institute, Fédération de Recherche CNRS 3104, 33 rue St. Leu, 80039 Amiens, France

ABSTRACT: We report a comprehensive multiscale model describing charge processes of Li–O_2 batteries. On the basis of a continuum approach, the present model combines mathematical descriptions of mass transport of soluble species (O_2, Li^+, LiO_2) and elementary reaction kinetics, which are assumed to be dependent on the morphology of the Li_2O_2 formed during discharge. The simulated charge curves are in agreement with previously reported experimental studies. The model along with the assumed reaction mechanisms provides physical explanations for the two-step charge profiles. Furthermore, it suggests that these charge profiles depend on the size of the Li_2O_2 particles, which are determined by the applied current density during discharge. Therefore, the model underlines the strong link between discharge and charge processes.

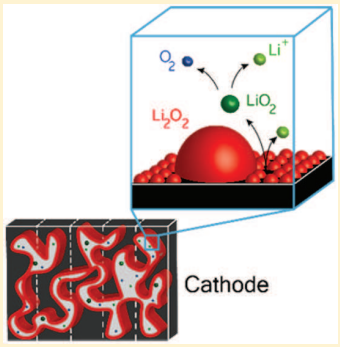

Li–O_2 batteries have attracted significant attention due to their high theoretical capacity up to ~3000 Wh/kg,[1] but they are still facing a large number of challenges which avoid their penetration in real applications. Their high charging voltage, which usually reaches 3.8 V and even more than 4 V, triggers problems such as poor round-trip efficiency and unfavorable parasitic reactions.[2] Unlike conventional lithium ion batteries (LIBs), the polarization of Li–O_2 batteries is very high, particularly during the charge process. This high polarization brings a potential gap as large as 1 V between charge and discharge, leading to an intrinsic loss of energy efficiency from source to end. Besides, it is reported that the commonly used carbon-based air electrodes are not stable above 3.5 V.[3] Carbon corrosion taking place at these high potentials not only deteriorates the coulombic efficiency but also releases CO_2 and then forms Li_2CO_3 during the subsequent discharge. Li_2CO_3 is an insulator, and it is stable within the potential window used for cycling; therefore, it is impossible to attain its complete removal, which leads to its accumulation and thus a gradual failure of the battery.[4] In short, lowering charging potential is preferential to ensure the durability of Li–O_2 batteries and therefore it is of high importance to develop a deeper understanding of the charging process. However, compared with discharge, the attention paid until now to understand the charge (or recharge) process of Li–O_2 batteries is very limited.

It is reported in literature that the charging of Li–O_2 batteries is a stepwise process, although exact potentials for each phenomena differ from one case to another.[5,6] There are few attempts based on experimental observations to explain the stepwise charge phenomenon in the literature. On the basis of in operando X-ray diffraction analysis, Ganapathy et al. suggested that the charge process starts with oxidation of amorphous Li_2O_2, followed by a layer-by-layer elimination of Li_2O_2 toroidal particles via a Li-deficient solid-solution reaction.[7] Lu et al. proposed a charging mechanism that associates the initial stage of charge to the Li^+ deintercalation from Li_2O_2 that results in the formation of LiO_2-like species on its surface, while the later stage is assigned to the oxidation of bulk Li_2O_2 particles to form Li^+ and O_2 via a two-phase transition.[8] Most of these opinions are qualitative speculations and they lack a deeper examination to verify the consistencies of the assumptions behind. From the modeling side, Ceder et al. proposed an alternative reaction pathway of crystalline Li_2O_2 via the formation of off-stoichiometric $Li_{2-x}O_2$ compound rather than direct decomposition,[9] while Dabrowski et al. related the two-step process to a mechanism with an initial peroxide-to-superoxide transition at lower potentials, followed by a later

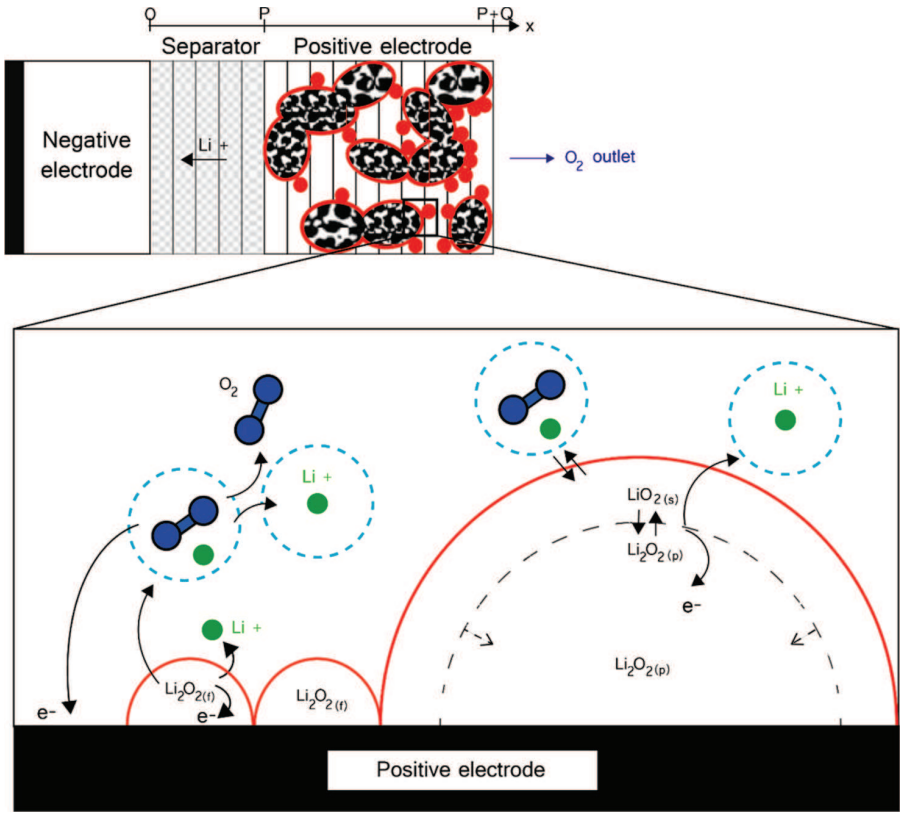

Figure 1. Schematic illustration of the charge mechanisms adopted in our model for thin-film (small hemispheres) and large Li_2O_2 large particles (large hemispheres).

release of O_2 as well as Li^+.[10] The above theoretical investigations are carried out on the atomic scale, where the impacts of mass transport and discharge product morphologies on the charge mechanism have been overlooked.

The initial conditions of the charge processes strongly depend on the discharge history, which determines the morphology and spatial distribution of the primary discharge product Li_2O_2. It is reported that the discharge of Li–O_2 batteries can go through different pathways.[11] The surface mechanism gives a passivating thin layer with a thickness of 5–10 nm, which is around the maximum electron tunneling distance according to DFT calculations,[12] while the solution-phase mechanism forms large particles up to several microns in size and which usually adopt a toroidal morphology.[13] These two mechanisms compete during the discharge and are highly dependent on the solvent properties as well as on the discharge rate.[14] Bazant et al. have postulated the existence of a critical current density at which the transition from large particles to small particles takes place, implying that thin-film and large particles will not coexist in the system.[13] However, Lau et al. disagree with this view because the results of their discharge model, which is based on the nucleation and growth of Li_2O_2, have shown the existence of a bimodal particle size distribution after full discharge with its peaks positioned at 47 and 170 nm.[15] The coexistence of the thin-film and large particles has also been experimentally confirmed indirectly by Zhai et al. because they found that the sizes of Li_2O_2 toroids did not change during the first step of charge.[5]

We propose a mechanistic model to investigate the impact of the Li_2O_2 morphology on the charge process. As far as we know, this is the first reported model providing a cohesive framework to explain the observed experimental features upon the Li–O_2 battery charge. As shown in Figure 1, we assume that the thin-film and the large particles coexist after discharge, which is the initial condition of our charge model. The thin film is assumed to be composed of small particles, and morphologies of both the thin-film and the large particles are assumed to be hemispherical. Moreover, different decomposition mechanisms are adopted for Li_2O_2 based on their particle sizes due to the following reasons: First, although the bulk Li_2O_2 is considered as an insulator, its surface can be metallic or semimetallic, as shown by theoretical calculations;[16] therefore, the electronic conductivity of Li_2O_2 particles can be a function of its particle size. Moreover, large particles show higher crystallinity than the thin film, and higher oxidation kinetics is expected for the more amorphous form.[17]

The elementary reactions involved in the modeled charge process are listed in Chart 1. Equation 5 holds for the Li^+ reduction to form Li at the negative electrode. At the positive electrode, for the large Li_2O_2 particles ($Li_2O_{2(p)}$), the oxidation starts with the deintercalation of Li^+ from its particle surface (eq 1), forming LiO_2-like species ($LiO_{2(s)}$). Then, the $LiO_{2(s)}$ is dissolved into the electrolyte in the form of ion pair (eq 4), noted as $LiO_{2(ip)}$, followed by a further oxidation on the electrode surface to produce Li^+ and O_2 (eq 3). For the thin-film Li_2O_2 particles ($Li_2O_{2(f)}$), a two-step decomposition mechanism is adopted where $LiO_{2(ip)}$ is produced directly by the oxidation of $Li_2O_{2(f)}$ (eq 2), followed by the subsequent oxidation of $LiO_{2(ip)}$. Because of the very fast decomposition of

Chart 1. Elementary Reactions Involving in the Charge Process in Our Model

$Li_2O_{2(p)} \rightarrow Li^+ + e^- + LiO_{2(s)}$	[1]
$Li_2O_{2(f)} \rightarrow Li^+ + e^- + LiO_{2(ip)}$	[2]
$LiO_{2(ip)} \rightarrow Li^+ + e^- + O_2$	[3]
$LiO_{2(s)} \rightarrow LiO_{2(ip)}$	[4]
$Li^+ + e^- \rightarrow Li_{(s)}$	[5]

$LiO_{2(ip)}$ during the third step of charge, the oxidation of $Li_2O_{2(f)}$ can be regarded as a one-step reaction involving two electrons.

For the electrochemical reactions at the positive electrode (eqs 1–3), the reaction rate is characterized by the local faradaic current density i^{far}

$$i_j^{far} = n_e F\left\{k_{fj}\prod_i c_i^{s_{i,j}} \exp\left(\frac{(1-\alpha)n_e F(\Psi-\Phi)}{RT}\right) - k_{bj}\prod_i c_i^{s_{i,j}} \exp\left(-\frac{-\alpha n_e F(\Psi-\Phi)}{RT}\right)\right\} \quad (6)$$

where c_i is the dimensionless concentration (activity) of species i, $s_{i,j}$ is the stoichiometric coefficient of species i in reaction j, n_e is the number of electrons transferred in the reaction, k_{fj} and k_{bj} are the heterogeneous rate constants, α is the charge-transfer coefficient, Ψ is the electrostatic potential in the electron-conductive phase (electrode), and Φ is the electrostatic potential in the electrolyte phase. Then, the cell potential is calculated with

$$U_{cell} = \Psi_{pos} - \Psi_{neg} \quad (7)$$

Under the galvanostatic condition, the total applied current (I_{input}) given in amperes, is as follows

$$I_{input} = \int_0^V \sum_j \frac{A_j}{V} \cdot i_j^{far}\, dv \quad (8)$$

where A_j is the active surface area of the electrochemical reaction j, i_j^{far} is the Faradaic current density ($A{\cdot}m^{-2}$) of the electrochemical reaction j, and V is the electrode volume. It is worth noting that Ψ as well as Φ are identical for all electrochemical reactions at the cathode. However, the value of A_j differs from one reaction to another due to the difference in mobility of the electro-active species. For immobile Li_2O_2 solids, either in the form of large or thin-film particles, the active surface area for their oxidation refers to the surface area of the particle, as the reactions happen at the particle/electrolyte interface. Thus for both morphologies the active surface areas are calculated with the following equations

$$A_p = 2\pi r_p^2 N_p V \quad (9)$$

$$A_f = 2\pi r_f^2 N_f V \quad (10)$$

where r_p and r_f are the radius of the large and thin-film particles, respectively, and N_p and N_f are the density (number per unit of electrode volume) of large and thin-film particles, respectively. The $LiO_{2(ip)}$ oxidation takes place mainly on the uncovered part of the electrode (e.g., carbon) by Li_2O_2; therefore, its corresponding active surface area ($A_{LiO_2(ip)}$) for the reaction is

$$A_{LiO_2(ip)} = A_C - \pi r_f^2 N_f V - \pi r_p^2 N_p V \quad (11)$$

where A_C is the electrode (carbon) surface area.

For the chemical reaction, that is, $LiO_{2(s)}$ dissolution (eq 4), the reaction rate is described by

$$v_4 = k_{f,4} A_{LiO_{2(s)}} - k_{b,4}\frac{C_{LiO_{2(ip)}}}{C_{LiO_{2(ip),ref}}} \quad (12)$$

where $k_{f,4}$ and $k_{b,4}$ are the kinetic rate constants for the forward and backward processes, respectively. $LiO_{2(s)}$, produced by the oxidation of the large Li_2O_2 particles (eq 1), forms a film over the large Li_2O_2 particles surface, and $A_{LiO_{2(s)}}$ is the surface area of $LiO_{2(s)}$, which is exposed to the electrolyte

$$A_{LiO_{2(s)}} = A_p\theta \quad (13)$$

where θ stands for the surface coverage of $LiO_{2(s)}$ on the Li_2O_2 large particles surface. The $LiO_{2(s)}$ film formed on the surface of the large Li_2O_2 particles may consist of multiple $LiO_{2(s)}$ layers. When the $LiO_{2(s)}$ film is a monolayer, its surface coverage over the large Li_2O_2 particles is determined from the ratio between the surface area of adsorbed $LiO_{2(s)}$ and the surface area of the large Li_2O_2 particles (Figure 2). The surface coverage is assumed to be 1 if the $LiO_{2(s)}$ consists of multiple layers.

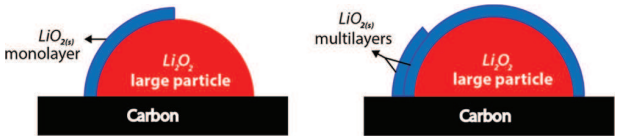

Figure 2. Schematics of the $LiO_{2(s)}$ formed on the surface of a large Li_2O_2 particle: To the left, a case is represented where the $LiO_{2(s)}$ monolayer covers less than the large Li_2O_2 particle surface ($\theta < 1$), and to the right, a case is represented where $LiO_{2(s)}$ completely covers the large Li_2O_2 particle surface and forms a multilayer ($\theta = 1$).

The mathematical criterion for the surface coverage by $LiO_{2(s)}$ on the large Li_2O_2 particles is then

$$\theta = \begin{cases} \dfrac{V_{LiO_2(s)}}{\delta N_p V 2\pi r_p^2}, & \dfrac{V_{LiO_2(s)}}{\delta} < N_p V 2\pi r_p^2 \\ 1, & \dfrac{V_{LiO_2(s)}}{\delta} \geq N_p V 2\pi r_p^2 \end{cases} \quad (14)$$

where $V_{LiO_{2(s)}}$ is the volume of the $LiO_{2(s)}$ calculated as a function of time by using eq 12 and eq S5 as follows

$$V_{LiO_{2(s)}}(t) = \omega_{LiO_{2(s)}} \int_0^t [v_1(t') - v_4(t')]\, dt' \quad (15)$$

Besides, the dissolution kinetics of the $LiO_{2(s)}$ formed over the large Li_2O_2 particles is assumed to be dependent on their particle size according to[18]

$$k_{f,4} = k^{\infty} \exp\left(\frac{2\sigma_{LiO_{2(s)}}\omega_{LiO_{2(s)}}}{RTr_p}\right) \quad (16)$$

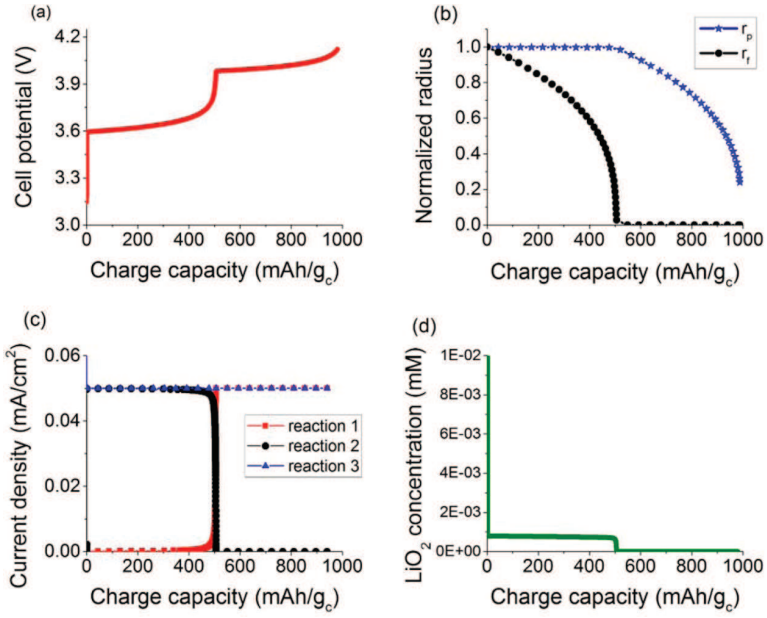

Figure 3. Simulated results of (a) potential evolution as a function of charge capacity. (b) Size evolution of large particles ($Li_2O_{2(p)}$) and small particles ($Li_2O_{2(f)}$) during the charge processes; the displayed sizes are normalized to the initial radius (75 and 7 nm for $Li_2O_{2(p)}$ and $Li_2O_{2(f)}$, respectively). (c) Evolution of Faradaic current densities due to the oxidation of $Li_2O_{2(p)}$ (red), $Li_2O_{2(f)}$ (black), and $LiO_{2(ip)}$(blue) as a function of the charge capacity. (d) Concentration of $LiO_{2(ip)}$ as a function of the charge capacity. All cell parameters are adapted from Zhai et al.,[5] and the assumed charge current in the simulation is equal to 0.1 mA/cm^2.

where k^{∞} is a prefactor, $\sigma_{LiO_{2(s)}}$ is the $LiO_{2(s)}$ surface tension, and $\omega_{LiO_{2(s)}}$ is the molar volume of $LiO_{2(s)}$.

For the electroactive species that are soluble in the electrolyte, namely, Li^+, O_2, and $LiO_{2(ip)}$, we follow our previous approach to solve their transport across the positive electrode as well as the separator.[14,19,20] It is assumed that the mass transport is governed by diffusion; therefore, transport of species i is described by the following equation

$$\frac{\partial(\varepsilon c_i)}{\partial t} = \frac{\partial}{\partial x}\left(\varepsilon^{\beta} D_0 \frac{\partial c_i}{\partial x}\right) + \gamma_i \tag{17}$$

where ε is the porosity of the positive electrode or the separator, β is the Bruggeman coefficient, D_0 is the bulk diffusion coefficient, and γ_i is the source term, standing for the consumption rate or generation rate of species. ε evolution during charge is calculated from the volume changes of large and thin-film Li_2O_2 particles (cf. Supporting Information). γ_i is obtained by summing up the consumption/formation rates of species i in each reaction

$$\gamma_i = \sum_j s_{ij} v_j \tag{18}$$

The evolution of the large Li_2O_2 particles volume during the charge is given by

$$V_p(t) = V_{p,0} + \omega_{Li_2O_2} \int_0^t \gamma_p(t) V \, dt \tag{19}$$

where $V_{p,0}$ represents the initial volume of the large Li_2O_2 particles. Under the assumption of isotropic volume change, the evolution of the large particles size is obtained as it follows

$$r_p(t) = \left(\frac{3}{2\pi N_p V} V_p(t)\right)^{1/3} \tag{20}$$

The evolution of the thin-film particles volume and size are calculated through a similar approach. Because Li_2O_2 is consumed during the charge, γ_p and γ_f are both negative; therefore, these rates will cause their particle sizes and surface areas to decrease along the charge process. Under the galvanostatic condition where the imposed current remains constant and thus by combining eqs 6−8, it is expected that the cell potential will increase during the charge processes due to the shrinking of the Li_2O_2 particles. Computational details of the simulations are provided in the Supporting Information.

Figure 3a shows that according to the simulated charge profile by using our model, the charge of a Li−O_2 battery is a two-step process. All used cell parameters are from the experimental setup reported by Zhai et al.[5] and are listed in Table S1. The initial radius of the large particles is 75 nm, which is adapted from Lau et al.,[15] while the radius of small particles is assumed to be 7 nm, which is close to the electron tunneling distance of Li_2O_2.[12,21] As shown in Figure 3b, during the initial stage of the charge process, decomposition of small particles takes place, which continues until its complete removal, and then the decomposition of large particles starts. This successive decomposition is in agreement with the stepwise behavior of the charge profile, which implies that small particle oxidation accounts for the plateau at lower potential in Figure 3a, while large particle oxidation is related to the plateau at higher potential. This phenomenon is also consistent with the evolution of faradaic current densities due to the oxidation reactions of $Li_2O_{2(f)}$, $Li_2O_{2(p)}$, and $LiO_{2(ip)}$ along the charge process (Figure 3c). Moreover, Figure 3c also shows that the current density due to the oxidation of $LiO_{2(ip)}$ always accounts for half of the total applied current density;

therefore, the $LiO_{2(ip)}$ concentration remains low throughout the charge process (Figure 3d). This steady oxidizing current density also causes the $LiO_{2(ip)}$ to decompose as soon as it is produced, which is in agreement with the fact that the $LiO_{2(ip)}$ has a short lifetime due to its fast kinetics.

Furthermore, the impacts of the discharge history, particularly the discharge rates on the charge processes, are investigated using our model. The first aspect of these history effects comes from the particle size distribution of Li_2O_2 produced after discharge. Usually, at higher discharge rates, it is expected to have larger proportion of the Li_2O_2 in the form of small particles (thin-film), whereas at lower rates Li_2O_2 get coalesced into large particles.[17,22] Therefore, the ratio between the total amount of large and small particles depends on the discharge rate. Figure 4a shows simulated charge curves with

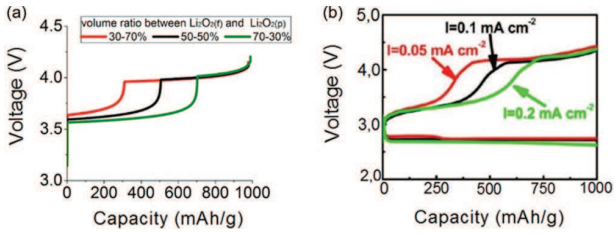

Figure 4. (a) Charge curves with different volume fraction of $Li_2O_{2(f)}$: 30% (red), 50% (black), 70% green (green), which is in agreement with (b) charge curves corresponding to different discharge current densities: 0.05 mA/cm^2 (red), 0.1 mA/cm^2 (black), and 0.2 mA/cm^2 (green). The charge current in all the cases is 0.1 mA/cm^2 and the capacities are normalized to mass of carbon in g. Panel b is reprinted with permission from ref 5.

different amount of small/large particles ratio, which illustrates that the capacity of the low potential plateau increases with the increase in the proportion of small particles. The simulation results are consistent with the experimental charge curves by Zhai et al., as shown in Figure 4b.

It is observed that the charge curves from experiments have smoother transition between the two charge plateaus, which may arise from the existence of a wider distribution of Li_2O_2 particle sizes, as suggested by Lau et al.[15] The oxidation kinetics during charge of Li−O_2 batteries has been shown to be dependent on the particle sizes of Li_2O_2 using our present charge model. Therefore, in the future, we intend to implement a detailed particle size distribution, which may produce smoother charge curves with even sloppier plateaus, as obtained in some experiments.[17] Moreover, we are developing a full cycle model by combining discharge model with the present charge model. Therefore, the initial configuration including the particle size distribution and spatial distribution for charge, which are estimated here, can be obtained as outputs from the discharge part.

An innovative model has been developed that simulates the charge process of Li−O_2 batteries by combining mass transport and elementary reaction kinetics. The model reproduces the stepwise charge profile of Li−O_2 cells, and it is shown to be a particle size-dependent mechanism, which is in good agreement with the experimental observations. Furthermore, the analyses of our model results suggest that the particle size distribution of Li_2O_2, which depends on the discharge history, has strong impacts on the charge processes. Therefore, controlling the discharge operation conditions can be an approach to improve the round-trip efficiency and cycle life, as reported in literature.[23] However, it is worth noting that the discharge capacity of the cell usually decreases with the increase in discharge rate. Thus there is always a trade-off between different aspects of cell performances, and modeling can be an efficient tool to find the good compromise.

■ ASSOCIATED CONTENT

Supporting Information

The Supporting Information is available free of charge on the ACS Publications website at DOI: 10.1021/acs.jpclett.6b01823.

Cell parameters implemented in the model, numerical method description, and model flowchart. (PDF)

■ AUTHOR INFORMATION

Corresponding Author

*E-mail: alejandro.franco@u-picardie.fr.

Notes

The authors declare no competing financial interest.

■ ACKNOWLEDGMENTS

Y.Y., V.T., and A.A.F. acknowledge Conseil Régional de Picardie and the European Regional Development Fund for the funding support through the project MASTERS. C.G. and A.A.F. are grateful to IRT Saint Exupéry for the financial support. A.T. and A.A.F. thank ALISTORE European Research Institute for A.T.'s Ph.D. grant. Dr. Charles Delacourt and Prof. Dominique Larcher at LRCS are acknowledged for helpful discussions.

■ REFERENCES

(1) Larcher, D.; Tarascon, J.-M. Towards Greener and More Sustainable Batteries for Electrical Energy Storage. *Nat. Chem.* **2014**, *7*, 19−29.

(2) Girishkumar, G.; McCloskey, B.; Luntz, A. C.; Swanson, S.; Wilcke, W. Lithium−Air Battery: Promise and Challenges. *J. Phys. Chem. Lett.* **2010**, *1*, 2193−2203.

(3) Bruce, P. G.; Freunberger, S. A.; Hardwick, L. J.; Tarascon, J.-M. Li-O_2 and Li-S Batteries with High Energy Storage. *Nat. Mater.* **2011**, *11*, 19−29.

(4) Lu, Y.-C.; Gallant, B. M.; Kwabi, D. G.; Harding, J. R.; Mitchell, R. R.; Whittingham, M. S.; Shao-Horn, Y. Lithium−oxygen Batteries: Bridging Mechanistic Understanding and Battery Performance. *Energy Environ. Sci.* **2013**, *6*, 750−768.

(5) Zhai, D.; Wang, H.-H.; Yang, J.; Lau, K. C.; Li, K.; Amine, K.; Curtiss, L. A. Disproportionation in Li−O_2 Batteries Based on a Large Surface Area Carbon Cathode. *J. Am. Chem. Soc.* **2013**, *135*, 15364−15372.

(6) McCloskey, B. D.; Valery, A.; Luntz, A. C.; Gowda, S. R.; Wallraff, G. M.; Garcia, J. M.; Mori, T.; Krupp, L. E. Combining Accurate O_2 and Li_2O_2 Assays to Separate Discharge and Charge Stability Limitations in Nonaqueous Li−O_2 Batteries. *J. Phys. Chem. Lett.* **2013**, *4*, 2989−2993.

(7) Ganapathy, S.; Adams, B. D.; Stenou, G.; Anastasaki, M. S.; Goubitz, K.; Miao, X.-F.; Nazar, L. F.; Wagemaker, M. Nature of Li_2O_2 Oxidation in a Li−O_2 Battery Revealed by Operando X-Ray Diffraction. *J. Am. Chem. Soc.* **2014**, *136*, 16335−16344.

(8) Lu, Y.-C.; Shao-Horn, Y. Probing the Reaction Kinetics of the Charge Reactions of Nonaqueous Li−O_2 Batteries. *J. Phys. Chem. Lett.* **2013**, *4*, 93−99.

(9) Kang, S.; Mo, Y.; Ong, S. P.; Ceder, G. A Facile Mechanism for Recharging Li_2O_2 in Li−O_2 Batteries. *Chem. Mater.* **2013**, *25*, 3328−3336.

(10) Dabrowski, T.; Ciacchi, L. C. Atomistic Modeling of the Charge Process in Lithium/Air Batteries. *J. Phys. Chem. C* **2015**, *119*, 25807−25817.
(11) Johnson, L.; Li, C.; Liu, Z.; Chen, Y.; Freunberger, S. A.; Ashok, P. C.; Praveen, B. B.; Dholakia, K.; Tarascon, J.-M.; Bruce, P. G. The Role of LiO_2 Solubility in O_2 Reduction in Aprotic Solvents and Its Consequences for Li−O_2 Batteries. *Nat. Chem.* **2014**, *6*, 1091−1099.
(12) Luntz, A. C.; Viswanathan, V.; Voss, J.; Varley, J. B.; Nørskov, J. K.; Scheffler, R.; Speidel, A. Tunneling and Polaron Charge Transport through Li_2O_2 in Li−O_2 Batteries. *J. Phys. Chem. Lett.* **2013**, *4*, 3494−3499.
(13) Horstmann, B.; Gallant, B.; Mitchell, R.; Bessler, W. G.; Shao-Horn, Y.; Bazant, M. Z. Rate-Dependent Morphology of Li_2O_2 Growth in Li-O_2 Batteries. *J. Phys. Chem. Lett.* **2013**, *4*, 4217−4222.
(14) Xue, K.-H.; McTurk, E.; Johnson, L.; Bruce, P. G.; Franco, A. A. A Comprehensive Model for Non-Aqueous Lithium Air Batteries Involving Different Reaction Mechanisms. *J. Electrochem. Soc.* **2015**, *162*, A614−A621.
(15) Lau, S.; Archer, L. A. Nucleation and Growth of Lithium Peroxide in the Li−O_2 Battery. *Nano Lett.* **2015**, *15*, 5995−6002.
(16) Radin, M. D.; Rodriguez, J. F.; Tian, F.; Siegel, D. J. Lithium Peroxide Surfaces Are Metallic, While Lithium Oxide Surfaces Are Not. *J. Am. Chem. Soc.* **2012**, *134*, 1093−1103.
(17) Adams, B. D.; Radtke, C.; Black, R.; Trudeau, M. L.; Zaghib, K.; Nazar, L. F. Current Density Dependence of Peroxide Formation in the Li−O_2 Battery and Its Effect on Charge. *Energy Environ. Sci.* **2013**, *6*, 1772−1778.
(18) Franco, A. A.; Tembely, M. Transient Multiscale Modeling of Aging Mechanisms in a PEFC Cathode. *J. Electrochem. Soc.* **2007**, *154*, B712−B723.
(19) Xue, K.-H.; Nguyen, T.-K.; Franco, A. A. Impact of the Cathode Microstructure on the Discharge Performance of Lithium Air Batteries: A Multiscale Model. *J. Electrochem. Soc.* **2014**, *161*, E3028−E3035.
(20) Franco, A. A.; Xue, K.-H. Carbon-Based Electrodes for Lithium Air Batteries: Scientific and Technological Challenges from a Modeling Perspective. *ECS J. Solid State Sci. Technol.* **2013**, *2*, M3084−M3100.
(21) Viswanathan, V.; Thygesen, K. S.; Hummelshøj, J. S.; Nørskov, J. K.; Girishkumar, G.; McCloskey, B. D.; Luntz, A. C. Electrical Conductivity in Li_2O_2 and Its Role in Determining Capacity Limitations in Non-Aqueous Li-O_2 Batteries. *J. Chem. Phys.* **2011**, *135*, 214704.
(22) Gallant, B. M.; Kwabi, D. G.; Mitchell, R. R.; Zhou, J.; Thompson, C. V.; Shao-Horn, Y. Influence of Li_2O_2 Morphology on Oxygen Reduction and Evolution Kinetics in Li−O_2 Batteries. *Energy Environ. Sci.* **2013**, *6*, 2518−2528.
(23) Mirzaeian, M.; Hall, P. J.; Sillars, F. B.; Fletcher, I.; Goldin, M. M.; Shitta-bey, G. O.; Jirandehi, H. F. The Effect of Operation Conditions on the Performance of Lithium/Oxygen Batteries. *J. Electrochem. Soc.* **2013**, *160*, A25−A30.